

Demonstration of ultrashort laser pulse amplification in plasmas by a counterpropagating pumping beam

Y. Ping, I. Geltner, N. J. Fisch, G. Shvets, and S. Suckewer
Princeton University, Princeton, New Jersey 08540

(Received 25 May 2000)

We experimentally demonstrated amplification of ultrashort laser pulses (200 fs pulses) in microcapillary plasmas by a counterpropagating pumping beam. Energy amplification as large as a factor of 5 was observed. Importantly, a nonlinear pump depletion regime must have been accessed, since the parameters support not only the amplification of the pulse, but an absolutely growing instability if the pump is not depleted. Further indication of accessing the nonlinear depletion is indicated by the relative insensitivity to the initial pulse energy.

PACS number(s): 52.40.Nk, 42.55.Vc, 32.80.Rm, 42.65.Dr

Raman compressors in gases and plasmas have been the object of study for considerable time [1–4]. Early work in plasmas recognized the difficulties of pulse compression in counterpropagating geometry because of the relatively narrow band nature of the Raman amplification and the instabilities of the amplified pulse itself. Narrow band amplification limits the temporal compression that can be achieved. One way around the narrow band amplification is through the use of collisional effects, although those effects tend also to reduce the efficiency [3]. Raman backscatter compressors, particularly in gases, have achieved compression at moderate energy and pulse lengths, from 0.1 to 10 J from tens of nanoseconds to tens of hundreds of picoseconds [5].

Recently, new effects were identified in the nonlinear behavior of ultrashort ultraintense pulses, which produce broadband growth in counterpropagating laser geometry [6,7]. In particular, the Raman backscatter effect when in the pump depletion regime [7] produces broadband amplification. For Raman backscatter, the efficiency is limited only by the Manley-Rowe relations for the three-wave interaction. In this regime, the pulse is shortened as it is amplified, because only the leading edge of the short pulse sees the pump.

The three-wave interaction between counterpropagating laser pulses and a plasma wave has been well-studied [8,9]. The plasma wave, with frequency ω_p ($\omega_p^2 = 4\pi e^2 n_e / m_e$), is ponderomotively driven by the periodic intensity pattern produced by the interface between the pumping pulse and the seed pulse. If the frequency detuning between the two pulses matches the plasma frequency ω_p , i.e., $\omega = \omega_{\text{pump}} - \omega_{\text{seed}}$, then the seed pulse can be amplified through Raman backscattering (RBS) instability of the pump. The goal of the present Rapid Communication is to show in a counterpropagating pulse geometry that significant amplification may be arranged for ultrashort pulses (200 fs). Of particular interest is to access the pump depletion regime.

Our experimental setup is shown in Fig. 1. A Ti:sapphire laser system is tuned to a wavelength $\lambda = 745$ nm with spectrum full width at half maximum ~ 4 nm and pulse duration ~ 200 fs. About $30 \mu\text{J}$ or less (of 5 mJ available) was used as the seed pulse in our experiments. The pumping pulse was provided by the second harmonic of a neodymium-doped yttrium aluminum garnet laser at $\lambda = 532$ nm with 150 mJ in 5 ns. The seed pulse and the pumping pulse were both fo-

cused onto the center of the microcapillary by an $f/25$ lens L_1 and an $f/8$ lens L_2 . The initial plasma was created inside the LiF microcapillary by ablation of the microcapillary wall by a low power nanosecond KrF laser. (The KrF laser can provide a beam up to 200 mJ in 20 ns at wavelength $\lambda = 248$ nm.) Lens L_3 is added to adjust the divergence of the KrF laser pulse (prepulse) in order to create a long and uniform plasma column in the microcapillary. The amplified laser pulse, propagating in the opposite direction to the pumping pulse, passes through mirrors M_2 and M_3 and is collected by lens L_4 onto the entrance slit of the air spectrometer.

The advantage of using a spectrometer in order to measure the seed pulse amplification is that any scattered signals at different wavelengths can easily be eliminated, hence the measured signal was not affected by other pulses. The entrance slit of the spectrometer was opened up to 1 mm to make sure that the entire subpicosecond pulse (seed pulse) was collected. The exit slit was fully opened (to about 3 mm), corresponding to spectrum width of about 5 nm, in order to fully cover the spectral width of the subpicosecond pulse. A photomultiplier with a 0.2 ns rise time was attached to the exit slit. Filters were inserted in front of the entrance slit to prevent saturation of the photomultiplier. The output

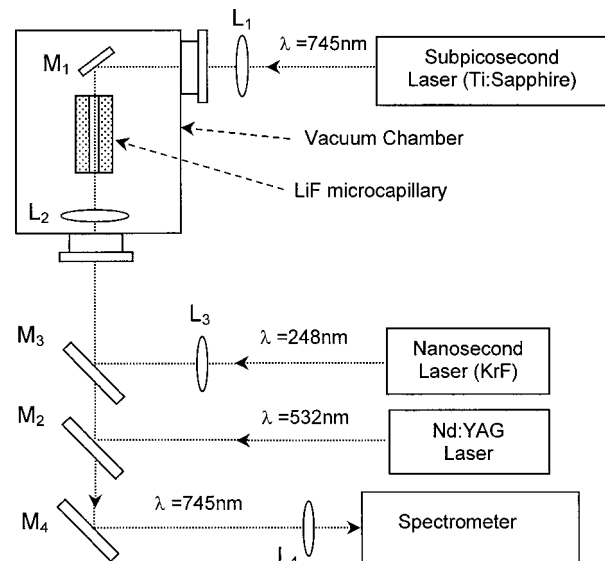


FIG. 1. Schematic of experimental arrangement.

signals were recorded with a fast oscilloscope. The signals, which are proportional to the total energy of the subpicosecond pulses, were integrated over the 5 nm range of its spectrum and over time $\tau \approx 2$ ns.

The diameter of the focus spots of the pumping pulse and the subpicosecond (seed) pulse (20 and 50 μm , respectively) are much smaller than the diameter of the microcapillary (250 μm). The larger diameter of the seed pulse was due to vacuum chamber limitations, hence the necessity of using an $f/25$ lens. Precise alignment of the pulses along the axis of the microcapillary was achieved by using a HeNe laser beam as a reference beam to fix the position of the axis, enabling proper alignment of all laser beams inside the microcapillary. As the distances between the target chamber and the lasers are very long (several meters), the precision of the alignment was very high. During the experiments, very fine adjustments of the mirrors M_1 and M_2 assured the overlapping of the pumping and seed pulses in the microcapillary plasma. The subpicosecond seed pulse is timed to interact with the front portion of the pumping pulse to avoid any changes in the initial plasma due to the heating process. This is done by finely tuning the relative timing between the two pulses by our timer system with accuracy of about 0.7 ns.

The three-wave interaction condition for experimental parameters $\omega_{\text{pump}} = 3.54 \times 10^{15}$ rad/sec and $\omega_{\text{seed}} = 2.53 \times 10^{15}$ rad/sec is satisfied by the plasma frequency $\omega_p = 1.01 \times 10^{15}$ rad/sec, corresponding to the electron density $n_e \approx 3 \times 10^{20} \text{ cm}^{-3}$. To create such high-density plasma, we chose a LiF microcapillary with a small diameter, $d = 250 \mu\text{m}$, in accordance to the estimated ablation rate of the wall [10] The KrF laser, with critical density $n_{e(\text{cr})} \approx 1.8 \times 10^{22} \text{ cm}^{-3}$ much higher than the required n_e , was very suitable for this purpose. The best matched plasma density was found by changing the delay between firing the KrF laser and subpicosecond laser, following the technique developed for choosing appropriate n_e for soft x-ray lasing generation in microcapillary plasma [11]. The delay between the prepulse and the seed pulse was scanned from 40 to 200 ns. The enhancement of the output signal was observed at delays between 40 to 100 ns, with the maximum amplification near 60 ns.

The seed pulse was aligned in such a way as to have no interaction with the wall, so there was no difference in the exit energy if the microcapillary was totally removed. Define V_o as the total exit energy in the seed pulse after interaction with the pumping beam in the microcapillary. Define V_i as the total exit energy in the seed pulse after traversing the microcapillary plasma but without the pumping pulse. Figure 2 shows the amplification ratio V_o/V_i versus the microcapillary length. Each point in Fig. 2 is an average of 20 shots, with the error bar calculated from the square root of standard variance. The energy of the laser pulses and the plasma conditions in the microcapillaries were kept as similar as possible for each microcapillary length. The results were obtained in two series of measurements (Expt 1 and Expt 2).

The results show the amplification increasing monotonically with length except for the $L = 2$ mm microcapillary. The much lower ratio V_o/V_i in Expt 1 is attributed to non-uniform filling of the microcapillary with plasma along its length, which was discovered during analysis of the data. One can see that a ratio V_o/V_i of ~ 5 was reached inside the $L = 3$ mm microcapillary. The maximum length of the mi-

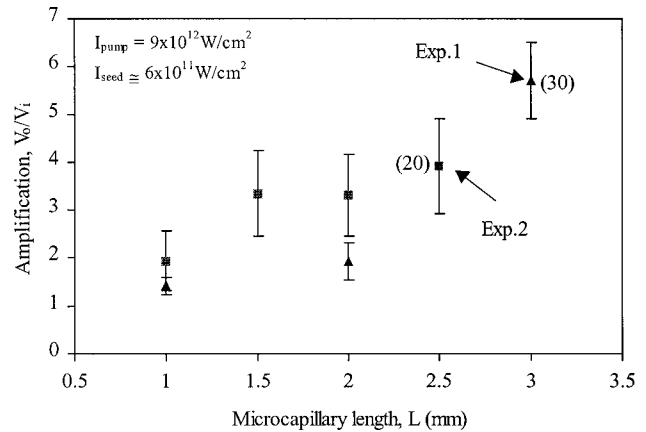


FIG. 2. Amplification of seed pulse intensity (squares and triangles) measured as a function of microcapillary lengths (microcapillary diameter ≈ 0.25 mm) for initial seed pulse intensity $I_{\text{seed}} = 6 \times 10^{11} \text{ W/cm}^2$, pump intensity $I_{\text{pump}} = 9 \times 10^{12} \text{ W/cm}^2$, and electron density in plasma $n_e = 3 \times 10^{20} \text{ cm}^{-3}$. In brackets are shown amplifications if pump and seed beams would be perfectly overlapped.

crocapillary was limited by the divergence of the pumping pulse. When the microcapillary length is more than 3 mm, the pumping pulse starts to interact with the wall, leading to the decrease of the amplification. The relatively large error is mainly due to the irreproducibility of the plasma and the intensity fluctuations ($\sim 10\%$) of the seed pulse and the pumping pulse. No significant change was observed in the subpicosecond pulse spectral energy distribution.

Recall that the seed pulse with a 50 μm diameter does not completely spatially overlap the 20 μm diameter focused pumping beam. If only the focused beam contributed to the amplification, then the overall amplification would have occurred through amplification of only $\frac{1}{6}$ of the seed pulse [$(20/50)^2 \rightarrow 16\%$]. That would indicate higher amplification by a factor of 6 in the overlapped portion; i.e., as high as 30, which was indicated in Fig. 2 by numbers in brackets. However, drawing this conclusion may not be totally correct because there is considerable nonfocused pump power overlapping the $\frac{5}{6}$ of the pulse that does not overlap the focused pump power. Since the linear Raman instability growth rate is proportional to pump amplitude rather than intensity, and since the nonfocused radiation can be encountered over a larger axial length, this nonoverlap term may not be negligible.

The intensity of the seed pulse was also varied by inserting filters between L_1 and the chamber window. It was found that the amplification ratio drops as the intensity of the seed pulse (I_{seed}) approaches the intensity of the pumping pulse (I_{pump}). A few data points of the amplification ratio versus I_{seed} for a 2 mm microcapillary are shown in Fig. 3. The horizontal error bar is due to the fluctuations in the seed pulse ($\sim 10\%$). When I_{seed} was significantly smaller than I_{pump} , the seed pulse was amplified more than three times (this corresponds to amplification 15 when assumed that only $\frac{1}{6}$ of the seed pulse is amplified.) As I_{seed} was increased and became close to I_{pump} , the ratio dropped to ~ 1 . So far we did not observe amplification when the initial I_{seed} exceeded I_{pump} .

An important aspect of pulse compression is the possibility of amplifying short seed pulses to orders of magnitude

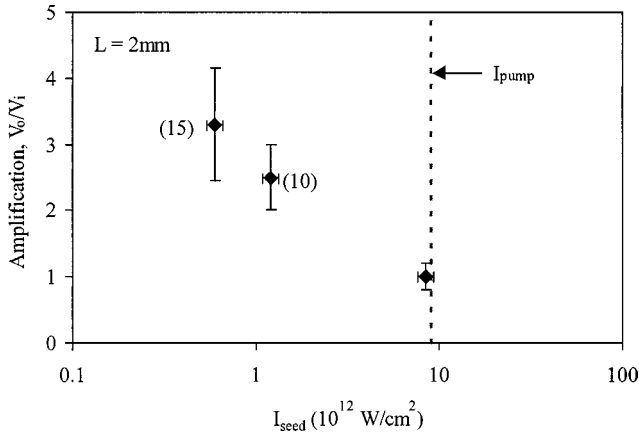


FIG. 3. Amplification of seed pulse intensity for its three different initial intensities ($I_{\text{seed}} \approx 0.6, 1.2,$ and $9 \times 10^{12} \text{ W/cm}^2$) for $I_{\text{pump}} \approx 9 \times 10^{12} \text{ W/cm}^2$ for 2 mm long microcapillary. All other parameters are as in Fig. 2.

higher intensities than the intensity of the pumping pulses. Note that for the results shown in Fig. 2, the energy of the seed pulse was about $2 \mu\text{J}$, for which the intensity was $6 \times 10^{11} \text{ W/cm}^2$ over the $50 \mu\text{m}$ diameter cross section. The pumping pulse intensity was $9 \times 10^{12} \text{ W/cm}^2$ at the focus ($20 \mu\text{m}$ diameter). However, if the full amplification can be attributed to only the 16% of the seed pulse overlapping with the pumping pulse, the maximum energy amplification for the 3 mm microcapillary would be 30 (see Fig. 2). For such energy amplification (assuming that the duration is not shortened), results in a power intensity reaching $1.8 \times 10^{13} \text{ W/cm}^2$, which would be larger than the intensity of the pumping pulse.

To summarize, the key experimental results are as follows: (i) There is an overall energy amplification of as much as a factor of 5. The pump when focused covers an area of about $\frac{1}{6}$ of the total seed pulse cross section. If all the amplification occurred in just this focused cross section, the amplification in the overlap region could be as much as 30; (ii) there is no spectral narrowing; (iii) there is an apparent saturation of the effect when the initial seed pulse intensity exceeds the pump intensity.

To understand these experimental findings, several factors need to be kept in mind. First, the high plasma density and its relatively low temperature (below $T_e = 200 \text{ eV}$) result in a very high rate of electron-ion collisions: at least 2.5 ps^{-1} . Electron-ion collisions result in the damping of the Langmuir plasma waves, thus explaining the absence of the spontaneous Raman backscattering (RBS) without the short pulse. A related effect is the inverse bremsstrahlung of the pump pulse, which has a damping rate smaller by a factor $n_{\text{crit}}/n_e = 12$. Collisional damping does not, however, prohibit the amplification of an ultrashort pulse, as observed in the experiment.

Now for half micron pump radiation focused to 10^{13} W/cm^2 , the vector potential is $a = 0.0014$. The linear growth distance for the power is about 0.4 mm, but the Rayleigh length over which the power is focused is only about 1 mm. Thus, the linear growth time, $1/\gamma$, is about 1.3 ps and $\gamma L/c$ gives about two growth rates over the focusing distance, which means that τ is about half a linear growth time, or less than 1 ps.

Given a small number of exponentiations, one would expect pulse lengthening from 200 fs to about a picosecond. This contradicts the experimental measurements of the pulse spectrum, which did not exhibit any narrowing. The lack of spectral narrowing can be explained in the following way. It is almost certain that there is a density inhomogeneity, axial or radial, sufficient to account for the broadband amplification. Because of the inhomogeneity, in different locations there will be different resonant frequencies. Since the 200 fs signal is about 100 backscattered radiation periods, a 2% variation in plasma density accounts for the 1% bandwidth in the backscattered radiation. Thus, the amplification is broadband enough to encompass the full signal spectral width with only rather small density variations in the radial or axial directions.

There is evidence of pump depletion, when considering the dependence of amplification of seed pulse on capillary length. In the linear regime, one would expect exponential variation with the capillary length. However, in the pump depletion regime, the dependence should be far milder. In fact, we do note that the amplification (or the output energy) appears to increase mildly with length. In the full pump depletion regime, we would again expect constant output energies; however, as we noted above, effects beyond our considerations here account for the relatively small fraction of the available input energy that is converted to backscatter energy. Thus, determining the precise amplification as a function of length is too speculative without further data. Nevertheless, the data are compatible with pump depletion, possibly over a small region, and clearly do not show the exponential growth that would be characteristic of the non-depletion regime.

In summary, a counterstreaming Raman amplifier in the subpicosecond regime was built and analyzed. In this regime, we expect to find both broadband amplification and pump depletion. The amplification is clearly broadband. Energy amplification factors of as much as 5 were recorded, with insensitivity to the specific input energies, as characteristic of pump depletion regimes rather than constant pump (exponential growth) regimes. Thus, it appears that Raman pump depletion behavior has been observed in the ultrashort pulse regime.

It is important to recognize significant caveats to the main conclusion, namely, that the pump depletion effect was observed for ultrashort pulses. First, there was insufficient time resolution to distinguish the expected spatiotemporal pulse evolution in this regime. Second, we did not demonstrate pulse intensity that significantly exceeded the pump intensity.

Developing a quantitative theory still remains a challenge because of nonideal effects, such as defocusing, density inhomogeneities driving the interaction off resonance, or damping effects. The present experiment should be regarded as a first step toward a demonstration of accessing the pump depletion regime with an ultrashort pulse. That goal is worthy enough to be accomplished carefully and in several steps, of which we trust this is the first.

We are thankful to Dr. A. Morozov for his help in the preparation of the experiment and N. Tkach for his technical support and for preparing the many electronic devices that were involved in the experiment. The experimental part of the work was supported by NSF Grant No. PHY-9732261.

- [1] M. Maier, W. Kaiser, and J. A. Giordmaine, *Phys. Rev. Lett.* **17**, 1275 (1966); *Phys. Rev.* **177**, 580 (1969).
- [2] J. R. Murray, J. Goldhar, D. Eimerl, and A. Szoke, *IEEE J. Quantum Electron.* **QE-15**, 342 (1979).
- [3] R. D. Milroy, C. E. Capjack, and C. R. James, *Phys. Fluids* **22**, 1922 (1979).
- [4] J. A. Caird, *IEEE J. Quantum Electron.* **QE-16**, 489 (1980).
- [5] H. Nishioka *et al.*, *IEEE J. Quantum Electron.* **QE-29**, 2251 (1993); E. Takahashi *et al.*, *Fusion Eng. Des.* **44**, 133 (1999).
- [6] G. Shvets, N. J. Fisch, A. Pukhov, and J. Meyer-ter-Vehn, *Phys. Rev. Lett.* **81**, 4879 (1989).
- [7] V. Malkin, G. Shvets, and N. J. Fisch, *Phys. Rev. Lett.* **82**, 4448 (1999).
- [8] W. L. Kruer, *The Physics of Laser Plasma Interactions* (Addison-Wesley, Reading, MA, 1988).
- [9] D. L. Bobroff and H. A. Haus, *J. Appl. Phys.* **38**, 390 (1967).
- [10] A. Goltsov, D. V. Korobkin, Y. Ping, and S. Suckewer, *J. Opt. Soc. Am. B* **17**, 868 (2000).
- [11] D. V. Korobkin, C. H. Nam, S. Suckewer, and A. Goltsov, *Phys. Rev. Lett.* **77**, 5206 (1996).